

A Euro-Mediterranean tree-ring reconstruction of the winter NAO index since 910 C.E.

Edward R. Cook¹ · Yochanan Kushnir¹ · Jason E. Smerdon¹ · A. Park Williams¹ · Kevin J. Anchukaitis² · Eugene R. Wahl³

Received: 9 November 2018 / Accepted: 18 February 2019 © Springer-Verlag GmbH Germany, part of Springer Nature 2019

Abstract

We develop a new reconstruction of the winter North Atlantic Oscillation (NAO) index using a network of 97 Euro-Mediterranean tree-ring series. The reconstruction covers the period 910–2018 C.E., making it the longest annually resolved estimate of winter NAO variability available. We use nested correlation-weighted principal components regression and the Maximum Entropy Bootstrap method to generate a 2400-member ensemble of reconstructions for estimating the final reconstruction and its quantile uncertainties. Extensive validation testing of the new reconstruction against data withheld from the calibration exercise demonstrates its skill. The skill level of the new reconstruction is also an improvement over two NAO reconstructions published earlier. Spectral analyses indicate that the new reconstruction behaves like a 'white noise' process with intermittent band-limited power, suggesting that the winter NAO is stochastically forced. The 'white noise' properties of our reconstruction are also shown to be consistent with the spectral properties of long instrumental NAO indices extending back to 1781 and NAO indices extracted from a large number of forced climate model runs covering the last millennium. In contrast, an annually resolved multi-proxy NAO reconstruction of comparable length, based in part on speleothem data, behaves more like externally forced 'red noise' process, which is inconsistent with our reconstruction, long observations, and forced model runs.

Keywords North Atlantic Oscillation · Euro-Mediterranean tree rings · Millennium reconstruction · Stochastic forcing

1 Introduction

The North Atlantic Oscillation (NAO) is one of the most important modes of atmospheric circulation in the Northern Hemisphere (NH) because of its association with wide-ranging impacts on climate variability (Hurrell et al. 2003). The phenomenon is expressed as monthly and longer variations in the location and strength of the permanent, large-scale circulation features of the North Atlantic, the low pressure

in the subpolar region and the subtropical anticyclone. These variations affect the distribution of surface and upper level winds, the path of storms over the North Atlantic and surrounding land areas, and hence the temperature and precipitation from North America to Eurasia and from the tropics to the Arctic (Hurrell et al. 2003). While recognition of the NAO in one form or another extends back more than two centuries (Stephenson et al. 2003), its importance as a mode of internal climate variability and forcing was not fully appreciated until the latter part of the twentieth century (van Loon and Rogers 1978; Rogers and van Loon 1979; Wallace and Gutzler 1981).

The NAO influences NH climate throughout most of the year (Barnston and Livesey 1987), especially in the North Atlantic sector (Hurrell and Deser 2009), but its strongest expression is in the boreal winter months of December through March (Hurrell 1995). While the NAO emerges as a feature on monthly to seasonal time scales, it has been known to exhibit marked decadal variability, as well as apparent multidecadal trends, the origin and cause of which

Published online: 05 March 2019



[☑] Edward R. Cook drdendro@ldeo.columbia.edu

Lamont-Doherty Earth Observatory, 61 Route 9W, Palisades, NY 10964, USA

School of Geography and Development and Laboratory of Tree-Ring Research, University of Arizona, Tucson, AZ 85721, USA

World Data Service for Paleoclimatology, NOAA National Centers for Environmental Information, 325 Broadway Street, Boulder, CO 80305, USA

are still debated (Kelley et al. 2012; Woollings et al. 2015). Given the importance of the NAO as a source of internal climate variability, there is also understandable concern about how it may be influenced by increasing greenhouse gas (GHG) forcing in the future (Osborn 2004; Rind et al. 2005; Dong et al. 2011). For all these reasons, there has been a keen interest in documenting and understanding the variability of the NAO, especially in winter and on decadal to centennial timescales, by extending estimates of the NAO index as far back in time as possible.

Monthly or seasonal NAO variability, particularly during winter, has historically been examined in the form of normalized pressure differences that reflect changes in the atmospheric pressure gradient between the Icelandic Low and Azores High centers of action, and suitably located land-based, instrumental, surface pressure records are typically used for this purpose. Jones et al. (1997) provide the longest such NAO index extending back to 1821 using early instrumental surface pressure observations from Gibraltar and Southwest Iceland. Earlier instrumental climate data from Europe have also been used to estimate monthly and seasonal NAO variability as far back as the late seventeenth century (Jones et al. 2003; Luterbacher et al. 1999; Cornes et al. 2013) and with seasonal resolution back to 1500 based on documentary evidence (Luterbacher et al. 2002a). To extend the NAO index any earlier than this time period requires well-dated and annually resolved climate proxies that are sensitive to the local climate influence of the NAO, such as those derived from tree rings and ice cores.

Several early attempts were made to reconstruct the annual winter NAO from long climate proxies located in the North Atlantic sector. These included the use of annual tree-ring records from Europe, Morocco, and North America (Cook et al. 1998; Stockton and Glueck 1999; Cullen et al. 2001) and annual ice core records from Greenland (Appenzeller et al. 1998), calibrated against instrumental data over a common time interval. However, these reconstructions were all found to be inconsistent with winter NAO indices derived from long European pressure, temperature, and precipitation records back to 1685 (Luterbacher et al. 1999), thus casting doubt on their validity (Schmutz et al. 2000).

The failure to consistently reconstruct the NAO from climate proxies prompted Cook et al. (2002) to revisit the NAO reconstruction problem using 107 tree-ring chronologies from Europe, Morocco, and Eastern North America and two ice-core accumulation records from Greenland. Additionally, a much longer instrumental winter NAO index based on long monthly surface pressure reconstructions beginning in 1780 (Jones et al. 1999) was used to statistically calibrate and validate the reconstruction. This enabled the use of a very long calibration period (1826–1979), which identified a statistically stable set of tree-ring and ice-core predictors for reconstruction. The data excluded from model

calibration (1781–1825) were then used to successfully validate the tree-ring and ice-core estimates of NAO. This also included successful comparisons to the Luterbacher et al. (2002a) winter NAO reconstructions back to 1500 based on sea level pressure reconstructions over the eastern North Atlantic and Europe (Luterbacher et al. 2002b). The result was a "well-verified" winter NAO index reconstruction (hereafter NAO $_{\rm Cook}$) covering the period 1400–1979 C.E. (Cook et al. 2002).

Since that time two longer NAO reconstructions have been produced that extend back into the beginning of the 2nd millennium C.E. The first is the Trouet et al. (2009) winter NAO index reconstruction (NAO_{Trouet}), which covers the period 1049-1995 C.E. This reconstruction is based on a speleothem record from Scotland (Proctor et al. 2000) and a long tree-ring chronology from Morocco (Esper et al. 2007), thus approximating the locations of the northern and southern poles of the instrumental NAO. The speleothem record was not annually resolved and also subject to dating uncertainties, so both proxy series were smoothed with a 30-year low-pass filter before they were normalized for NAO index calculation. The resulting NAO_{Trougt} reconstruction contained a remarkably persistent positive NAO phase throughout most of the medieval era from the 11th to the fourteenth centuries. This result has been supported by more recent analyses of multiple speleothems from the North Atlantic sector (Wassenburg et al. 2013; Baker et al. 2015; Deininger et al. 2017). The Proctor et al. (2000) and Baker et al. (2015) speleothems are nevertheless not fully independent.

More recently, Ortega et al. (2015) developed an annually resolved winter NAO index reconstruction based on a candidate network of 48 proxy records comprising treering data from Europe, Morocco, North America, ice cores from Greenland, and several lake-sediment and speleothem records. This set of proxies was then reduced to nine final winter NAO predictors (5 ice-core, 2 tree-ring, 2 speleothem records) using a 'model-constrained' method in which climate model reanalyses were used to "guarantee realistic NAO teleconnections" in the selection of the proxies (Ortega et al. 2015). The resulting winter NAO index reconstruction (NAO_{Ortega}) covers the period 1049–1969 C.E., thus making it possible to compare NAO_{Ortega} to NAO_{Trouet} during the medieval period. Ortega et al. (2015) found "no persistent positive NAO during the medieval period", thus calling into question the primary NAO_{Trouet} finding.

Here we present a new winter NAO index reconstruction extending back to 910 C.E. based on a Euro-Mediterranean tree-ring network used previously to produce the Old World Drought Atlas (OWDA) (Cook et al. 2015). Our use of this predominantly moisture-sensitive tree-ring network for winter NAO reconstruction intentionally exploits the known hydroclimatic sensitivity of the Euro-Mediterranean region



to winter NAO variability and forcing (Hurrell 1995; Trigo et al. 2002; Lopez-Moreno and Vincente-Serrano 2008), with the added value of extending the NAO reconstruction well back into medieval times using the long tree-ring chronologies present in the network. In so doing, we gain important new insights into the long-term properties of winter NAO variability over the Euro-Mediterranean region.

2 Data and methods

2.1 Data

Our winter NAO index reconstruction is for the extended winter (December-March; DJFM) season when the NAO is most energetic (Barnston and Livesey 1987; Hurrell 1995). The instrumental NAO index used for calibration comes from the Jones et al. (1999) monthly sea level pressure (SLP) reconstructions based on a network of 51 long SLP records distributed evenly over Europe. This index (NAO_{Iones}) covers the period 1781–1995 and is the same target variable used by Cook et al. (2002) to produce the NAO_{Cook} reconstruction. NAO_{Jones} is an extension of the longest 2-point NAO index based on SLP observations from Gibraltar and Southwest Iceland (Jones et al. 1997), which for winter season values are complete from 1824 to the present (https://crudata.uea. ac.uk/cru/data/nao/). The two series are shown in Fig. 1 and have a correlation of 0.96 over the 1824-1995 common period, thus making NAO_{Jones} highly suitable for use as the winter NAO index target variable for reconstruction.

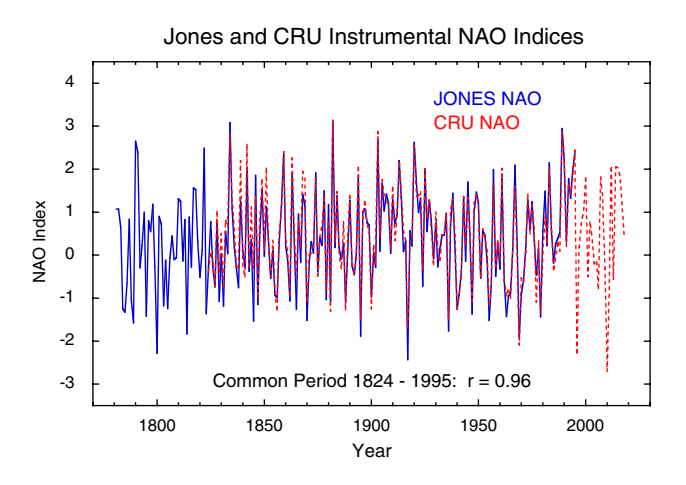


Fig. 1 Jones et al. (1999) winter NAO index from 1781 to 1995 (blue) extracted from monthly pressure field reconstructions for Europe compared to the 2-point CRU Gibraltar-Southwest Iceland winter NAO index (https://crudata.uea.ac.uk/cru/data/nao/) from 1824 to present (red). Over the period of overlap, the two indices are extremely similar, thus making the longer Jones index (NAO_{Jones}) appropriate to use as the target variable for reconstruction

Unlike NAO_{Cook}, our new reconstruction herein is based on the longest 97 tree-ring chronologies from the original 106-chronology OWDA tree-ring network (Cook et al. 2015). Using this proven network of moisture-sensitive treering series, we anticipate a more accurate reconstruction of the winter NAO due to its strong spatiotemporal influence on hydroclimatic variability over the Euro-Mediterranean region. The hydroclimatic signal associated with the winter NAO has been well documented by Trigo et al. (2002) and Lopez-Moreno and Vincente-Serrano (2008). Convincing NAO dependences in the OWDA have also been identified in Baek et al. (2017) (see Figs. 6 and 7 in that paper). The winter NAO influence on soil moisture content and recharge serves as the bridge that links winter NAO variability to tree growth during the following spring-summer growing season months. Tree growth is not only dependent on precipitation that falls during the concurrent growing season, but it can also depend strongly on antecedent rainfall that recharges the soil moisture reservoir prior to the onset of tree growth. Such winter moisture delivery over much of the European domain is controlled in part by the winter NAO.

The development of the OWDA tree-ring network is described in considerable detail in the Supplementary Materials of Cook et al. (2015). It is a multi-species network of tree-ring series that serves to reduce species-level biases in the reconstruction of climate from tree rings (García-Suáreza et al. 2009; Pederson et al. 2013). In producing the tree-ring chronologies from the raw data measurements great attention was paid to the preservation of low-frequency variability at timescales > 100 years. See Cook et al. (2015, Supplementary Materials) for details. Additionally, autoregressive (AR) modeling was applied to the tree-ring and the instrumental NAO data prior to reconstruction to closely match the overall spectral properties of the tree-ring reconstruction relative to the target NAO series (Meko 1981; Cook et al. 1999).

In order to compare observations and reconstructions of the NAO against simulations from long forced climate model simulations, we calculated the NAO index from 8 models used in the third phase of the Paleo Modelling Intercomparison Project (PMIP3; Taylor et al. 2012) lastmillennium experiment. The simulations cover the period from 850 to 1850 CE and use forcing estimates for solar variability, orbital parameters, vegetation, volcanic eruptions, and greenhouse gases (Schmidt et al. 2012). We extend the last-millennium experiments to 2005 using the historical simulations for each of the PMIP3 models from the accompanying fifth phase of the Coupled Model Intercomparison Project (CMIP5; Taylor et al. 2012). Here, we follow Gómez-Navarro and Zorita (2013) and calculate the model winter NAO as the leading principal component of the area-weighted December-March mean SLP over the North Atlantic (20–80°N, 90°W–40°E). For models with



multiple ensemble members, we calculate and plot the mean spectrum of the ensemble.

2.2 Reconstruction method

We use principal components regression (PCR; Cook et al. 1999) to reconstruct past NAO variability from our tree-ring network with reconstruction ensemble estimation done for uncertainty estimation using the Maximum Entropy Bootstrap (MEB; Vinod 2006; Cook et al. 2013a). As described in Cook et al. (1999), PCR can be applied using a simple correlation threshold (e.g., the 90% significance level) for selecting tree-ring predictors from a larger candidate pool. This hard threshold method of accepting or rejecting candidate predictors (similar to specifying an F-level for entry of variables in classical stepwise regression; Efroymson 1960) can work very well in practice, but it potentially loses useful climate information by rejecting candidate predictors that do not reach a specified significance threshold for correlation, even if marginally so. This issue can be avoided as described below.

Instead of a binary threshold for predictor variable selection, the method used here incorporates covariance between the tree-ring chronologies and the climate target in PCR by first weighting each tree-ring chronology by some power of its correlation over the calibration period with the climate variable being reconstructed (Cook et al. 2010, 2013a, b). This is succinctly expressed as:

$$wTR = uTR * r^p,$$

where uTR is the unweighted tree-ring chronology in normalized N[0,1] form over the calibration period, r is its calibration-period absolute correlation with the climate variable being reconstructed, p is some power weighting applied to r, and wTR is the resulting correlation-weighted chronology. The weighting thus transforms the correlation matrix of tree rings into a covariance matrix that emphasizes the more heavily weighted (better correlated with climate) treering series. PCR is then conducted using this correlation-weighted covariance matrix. See Cook et al. (2010) for its first use in drought atlas development.

There is no a priori reason why any particular power weighting, p, should be optimal. Thus, a range of powers is suggested. Here we use eight powers: $\{0, 0.1, 0.25, 0.5, 0.67, 1.0, 1.5, 2.0\}$. See Cook et al. (2013b) for the functional forms of these correlation weightings. These transformations are monotonic, continuous, and cover the full range of weightings as a function of r and chosen p. When p=0, wTR=uTR. A p=1.0 indicates a linear weighting by the simple correlation and p=2.0 indicates a weighting by the square of the correlation. Both have intuitively appealing interpretations regarding relationships between variables, and simple correlation weighting (p=1.0) has been used

in previous climate reconstructions (e.g., Smerdon et al. 2015; Tierney et al. 2015). PCA applied to each correlation-weighted covariance matrix thus produces a set of PCs that are weighted differentially by the climate variable being reconstructed. Run this way, PCR produces an ensemble of eight reconstructions that can be compared and pooled into an ensemble mean reconstruction. This has been done for the drought atlases produced by Cook et al. (2015), Palmer et al. (2015), and Stahle et al. (2016). Correlation-weighted PCR is used in this way here as well.

A drawback of PCR is the way it is limited to the common period of the tree-ring predictors used for reconstruction, with the shortest common period having the largest number of predictors. However, the tree-ring chronologies in the OWDA network have greatly varying lengths. In order to take full advantage of the longer tree-ring chronologies as predictors, and thus produce the longest reconstruction possible, PCR is applied in a stepped nested fashion to allow the reconstruction to be extended back in time as shorter tree-ring chronologies drop out of the model. The tree-ring PCs and regression model are recalculated with each change in tree-ring sample size and length, and the skill of each new model is evaluated. This nested reconstruction method was used for the Cook et al. (2002) NAO reconstruction and is similar to the nesting procedure used by Luterbacher et al. (1999, 2002a) to reconstruct the winter NAO index using early European instrumental records of varying lengths. It has also been used in a number of other contexts, including reconstruction of Northern Hemisphere mean temperature (cf. Wahl and Ammann 2007). Of the 106 OWDA tree-ring chronologies, 97 begin on or before 1700 and this is the beginning year of the first (or shortest) reconstruction nest.

2.3 Reconstruction calibration/validation tests

The correlation-weighted PCR reconstructions are assessed for skill using the calibration/validation tests described in Cook et al. (1999) and used for the NAO reconstruction in Cook et al. (2002). For consistency with NAO_{Cook} we again use the NAO_{Jones} data for calibration (1826–1989) and validation (1781–1825) testing. The metrics used to evaluate skill are the calibration period coefficient of determination or R² (CRSQ), the validation period square of the Pearson correlation, or r² (VRSQ), the reduction of error statistic (VRE), and the coefficient of efficiency (VCE) (Cook et al. 1999). By convention, if r < 0 in calculating VRSQ, the negative sign is assigned to VRSQ to indicate that the reconstruction has no skill by this measure. And by their formulations, VRE and VCE can be negative as well, which again indicates a lack of skill in the reconstructed values. VCE nevertheless can never be greater than VRSQ or VRE (Cook et al. 1999), which means that it is the hardest of the three skill statistics to pass.



Validation testing is performed within the PCR framework by comparing the tree-ring estimates to the instrumental data withheld from the calibration exercise, in this case the 1781-1825 NAO_{Iones} data. Validation testing on new data (sensu Berk 1984) is also performed here using the NAO index reconstructions of Luterbacher et al. (2002a) based on a mixture of early monthly instrumental climate data (pressure, temperature, precipitation) back to 1659 (NAO_{Lut1}). Seasonal NAO estimates based on documentary climate data are also available for testing from 1500 to 1658 (NAO_{Lut2}). Based on the analyses of Jones et al. (2003), these reconstructions are likely to additionally contain surface climate effects not related to NAO forcing alone because they are not based solely on atmospheric pressure data. This makes the non-SLP climate variables less ideal for use in reconstructing the NAO (Jones et al. 2003). The same criticism can be made of tree-ring data, but as will be shown, the judicious use of AR modeling (Meko 1981) has substantially corrected for differences in spectral shape between the target winter NAO index and the tree-ring data used as predictors in PCR.

2.4 Ensemble generation using the Maximum Entropy Bootstrap

It is possible to increase the ensemble size beyond the eight correlation-weighted reconstructions described above by using the MEB. Among all available bootstrap resampling methods, the MEB is unique in its ability to preserve, in a large sample sense, the full statistical properties of autocorrelated, and even non-stationary, time series that are commonly encountered in economics and climate science. MEB resampling satisfies the ergodic and central limit theorems, while at the same time preserving the 'data shape' (Vinod 2006) or temporal history of the data being resampled. This latter property enables the development of climate reconstruction ensembles in a simple, direct way by using the MEB resampled tree-ring series as if they were the original data. In climate science, the MEB has been used to model the uncertainties associated with monsoon onset and withdrawal in Thailand (Cook and Buckley 2009), uncertainties in the reconstruction of Indus River discharge estimated from tree rings (Cook et al. 2013a), and as a multivariate weather generator (Srivastav and Simonovic 2015).

MEB is applied here to randomly perturb the predictor and predictand data that enter into the correlation-weighted PCA part of PCR. Perturbing both the predictors and predictand admits the presence of unobserved error across all variables, which is a realistic assumption for both tree-ring series and the climate data used herein. It thus considers the climate reconstruction problem to be akin to an 'errors-invariables' problem with error on both sides of the model (Wonnocott and Wonnocott 1979). Here the error variances are assumed unknown and the MEB is used to compensate

for this lack of information by adding random variability to the input variables that go into PCR. Using the MEB this way, each of the eight correlation-weighted winter NAO reconstructions had 300 MEB reconstructions produced, producing a total of 2400 pseudo-reconstructions for estimating the reconstruction uncertainties.

The level of MEB perturbation applied to the predictor and predictand data in PCR can be assessed by calculating the differences between the 'true' PCR reconstruction of the winter NAO index, as defined by the median of the 2400 MEB reconstructions, and each of the 2400 MEB reconstructions themselves year by year. In so doing, the effect of the MEB perturbations was found to average about one-third (33%) the amplitude of the 'true' values, a level sufficient to generally exceed the 90% theoretical parametric regression uncertainties based on the Student's t-distribution (Olive 2007; Cook et al. 2013a). Additionally, the MEB uncertainties can be asymmetric, which is not possible for those based on the parametric estimates. The MEB applied this way can also produce uncertainties with coverage comparable to the 90% credible intervals produced by Bayesian regression (Rao et al. 2018).

It is conceivable that MEB, which conditions the perturbations on the specific time series incorporated, will underestimate the full nature of the uncertainties involved, both in terms of the proxy evidence and the calibration target information. However, this general issue is inherent in all the aforementioned methods used to evaluate prediction intervals. Based on the resampling and amplitude properties mentioned, we therefore find MEB to be an appropriate generalization of the classical t-distribution approach and empirically comparable to Bayesian estimation of the climate posterior, and thus it represents a reasonable approach to use for uncertainty estimation.

3 Results

The calibration/validation results for the eight NAO reconstructions are provided in Table 1. They represent only the nested models based on all 97 available chronologies. This is for the first and best replicated nest beginning in 1700 in each case. As noted previously, there is no reason why any particular level of correlation weighting should be optimal a priori, and this is apparent in the range of calibration/validation statistics shown. The calibration period CRSQ ranges from 0.412 to 0.506 and the most rigorous validation period VCE ranges from 0.121 to 0.396. The latter are all positive, which indicates some reconstruction skill in all eight models, but the p = 0, 0.50, and 0.67 weightings verify the best. This confirms that no single correlation-weighting is optimal, and it thus justifies the use of ensemble averages as was done for the OWDA (Cook et al. 2015). The calibration/



Table 1 Calibration/validation results for the eight correlation-weighted reconstructions of the winter (DJFM) NAO index

POWER	CRSQ	VRSQ	VRE	VCE
0.00	0.459	0.400	0.404	0.391
0.10	0.473	0.301	0.312	0.298
0.25	0.470	0.294	0.305	0.290
0.50	0.495	0.390	0.397	0.384
0.67	0.506	0.431	0.409	0.396
1.00	0.493	0.392	0.350	0.336
1.50	0.449	0.197	0.140	0.121
2.00	0.412	0.270	0.284	0.269
NAO _{Set}	0.524	0.382	0.387	0.374

The weighting is done as some power of \mathbf{r} ($\mathbf{r}^{\mathbf{p}}$), where \mathbf{r} is the correlation of each tree-ring chronology with the climate variable being reconstructed and \mathbf{p} is the power. See the text for details. The NAO_{Jones} index is the target variable for reconstruction from the OWDA tree-ring network using a similar calibration (1826–1989) and an identical validation (1781–1825) period to those used by Cook et al. (2002). Statistics for the 8-member ensemble mean set, NAO_{Set}, are in bold at the bottom

CRSQ calibration period R-squared, VRSQ validation period Pearson correlation squared, VRE validation reduction of error, VCE validation coefficient of efficiency

validation statistics for the 8-member ensemble set (NAO_{Set}) mean is provided in the last row. The average correlation between the eight ensemble members is 0.86, thus indicating relatively modest differences between reconstructions produced by the correlation weighting. The ensemble mean reconstruction has a larger CRSQ than any of the individual models, but the validation statistics do not improve proportionately and fall more towards the mid-range values of the individual models. This result is consistent with drought atlas ensemble average calibration/validation results, e.g., for the OWDA.

Additional calibration/validation tests of NAO_{Set} were conducted using NAO_{Lut1} and NAO_{Lut2} as reconstruction targets (Table 2). For comparison, the NAO_{Ortega} and NAO_{Cook} reconstructions were also tested for skill against the NAO_{Lut1} and NAO_{Lut2} reconstructions. NAO_{Ortega} differs from NAO_{Set} and NAO_{Cook} because the former is for the DJF winter season, while the latter are for the DJFM season. Both NAO_{Ortega} and NAO_{Cook} also differ from NAO_{Set} through their use of North American tree-ring and Greenland icecore data. The NAO_{Ortega} reconstruction in particular relies heavily on ice-core data and also includes two speleothem records. The exclusive use of the OWDA tree-ring chronologies focuses the NAO_{Set} reconstruction on Europe, thus making it more likely to compare well with NAO_{Lut1} and NAO_{Lut2} than either NAO_{Ortega} or NAO_{Cook}. Even so, these latter comparisons are useful because both NAO Ortega and NAO_{Cook} have been promoted as valid expressions of winter NAO variability and both have been compared against other

Table 2 Calibration/validation comparisons of the ensemble-based winter NAO reconstruction derived from the OWDA tree-ring network (NAO $_{\rm Set}$) and those of Ortega et al. (2015) (NAO $_{\rm Ortega}$) and Cook et al. (2002) (NAO $_{\rm Cook}$)

NAO RECON	CRSQ	VRSQ	VRE	VCE			
NAO _{Lut1} validation period: 1781–1822							
NAO _{Set}	0.278	0.426	0.435	0.420			
NAO _{Ortega}	0.223	0.158	0.205	0.109			
NAO_{Cook}	0.381	0.249	0.016	0.000			
NAO _{Lut1} validation period: 1659–1822							
NAO _{Set}	0.278	0.266	0.259	0.258			
NAO_{Ortega}	0.223	0.132	0.159	0.036			
NAO_{Cook}	0.381	0.244	0.181	0.181			
NAO _{Lut2} validation period: 1500–1658							
NAO _{Set}	0.278	0.192	0.152	0.152			
NAO_{Ortega}	0.223	0.000	-0.255	-0.255			
NAO_{Cook}	0.381	0.057	-0.169	-0.189			

The Luterbacher et al. (2002a) monthly (1659–2001) and seasonal (1500–1658) NAO reconstructions (NAO $_{Lut1}$ and NAO $_{Lut2}$, respectively) are used for calibration and validation. The period common to all series is 1500–1969, with the end year determined by the NAO $_{Ortega}$ reconstruction. The calibration period is 1823–1969 and the three validation periods are based on the same calibration model. The 1781–1822 and 1659–1822 validation period tests are based on a DJFM winter season calibration using the monthly NAO $_{Lut1}$ reconstruction. For the 1500–1658 validation period tests, only the DJF winter season is available for NAO $_{Lut2}$

CRSQ calibration period R-squared, VRSQ validation period Pearson correlation squared, VRE validation reduction of error, VCE validation coefficient of efficiency

NAO reconstructions available at the time of their respective publications.

The calibration and validation periods used in this second level of testing differ slightly from those in Table 1. For NAO $_{\rm Lut1}$ the calibration period is 1823–1969 because the end year of NAO $_{\rm Ortega}$ is 1969 and the validation tests reported by Ortega et al. (2015) used data that end in 1822. Thus, different validation periods were chosen for comparing NAO $_{\rm Set}$ to NAO $_{\rm Lut1}$: 1781–1822 and 1659–1822. The former is common to NAO $_{\rm Jones}$ and NAO $_{\rm Lut1}$. The latter provides a much longer interval for validation testing and is the same as that used by Ortega et al. (2015). For comparisons with the NAO $_{\rm Lut2}$ data, the NAO $_{\rm Lut1}$ data are used again for calibration from 1823 to 1969 and the 1500–1658 NAO $_{\rm Lut2}$ data are used for validation.

Table 2 provides the results using NAO_{Lut1} and NAO_{Lut2} as targets for both calibrating and validating NAO_{Set}, NAO_{Ortega}, and NAO_{Cook}. The calibration results are based on the same NAO_{Lut1} data and are therefore identical across all three validation tests. The order of calibrated variance (CRSQ) favors NAO_{Cook}, followed by NAO_{Set} and NAO_{Ortega}. Differences in NAO_{Jones} and NAO_{Lut1} over the calibration period must be responsible for the decline in



CRSQ for NAO_{Set} from Tables 1 and 2. Yet, the validation statistics for NAO_{Set} in Table 2 are better than in Table 1, indicating that the weaker calibration based on NAO_{Lut1} has not resulted in any loss of reconstruction skill in NAO_{Set}. In contrast, NAO_{Set} outperforms both NAO_{Ortega}, and NAO_{Cook} in all three validation tests by clear margins. Thus, taken at face value, the collective validation test results indicate that NAO_{Set} is likely to be more skillful than NAO_{Ortega} and NAO_{Cook} at describing the winter NAO impact on climate over Europe.

3.1 The final NAO reconstruction

The final reconstruction produced and evaluated here is NAO_{Med} , the median of all 2400 MEB reconstructions. NAO_{Med} is virtually identical to NAO_{Set} ($r\!=\!0.995$ between them), which allows the previous NAO_{Set} validation test results in Table 2 to still apply, with the added benefit that the 2400 MEB reconstructions can be used to estimate the NAO_{Med} reconstruction uncertainties. We plot NAO_{Med} and NAO_{Jones} together in Fig. 2a for visual comparison

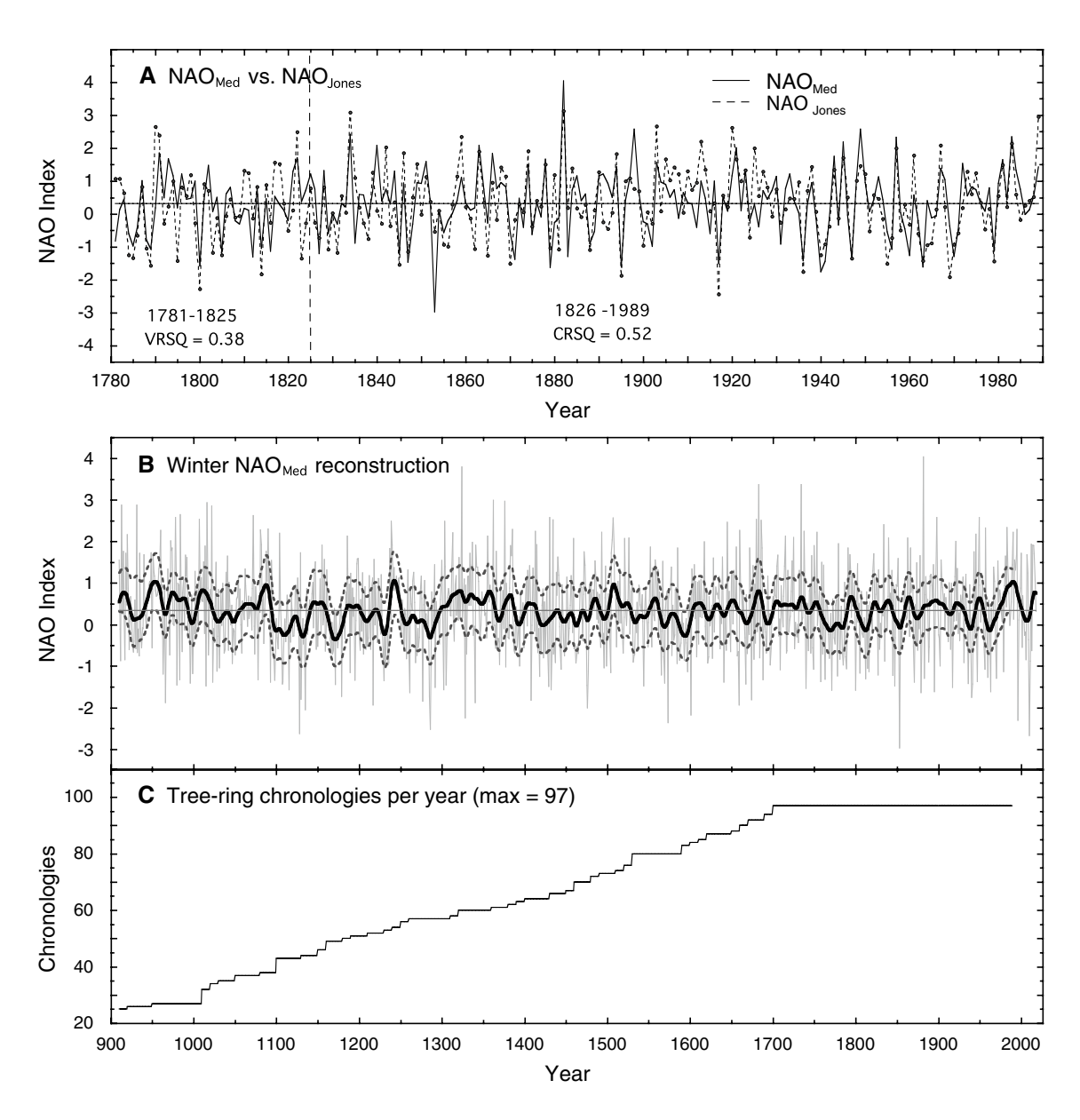


Fig. 2 The NAO $_{\mathrm{Med}}$ reconstruction is compared to the NAO $_{\mathrm{Jones}}$ record over the calibration (1826–1989) and validation (1781–1825) periods (**a**). The calibration (CRSQ) and validation (VRSQ) statistics are shown. The annually resolved NAO $_{\mathrm{Med}}$ reconstruction since 910 C.E. with 20-year low-pass smoothing and 90% quantile uncertainties are shown in **b**. The reconstruction has been extended from

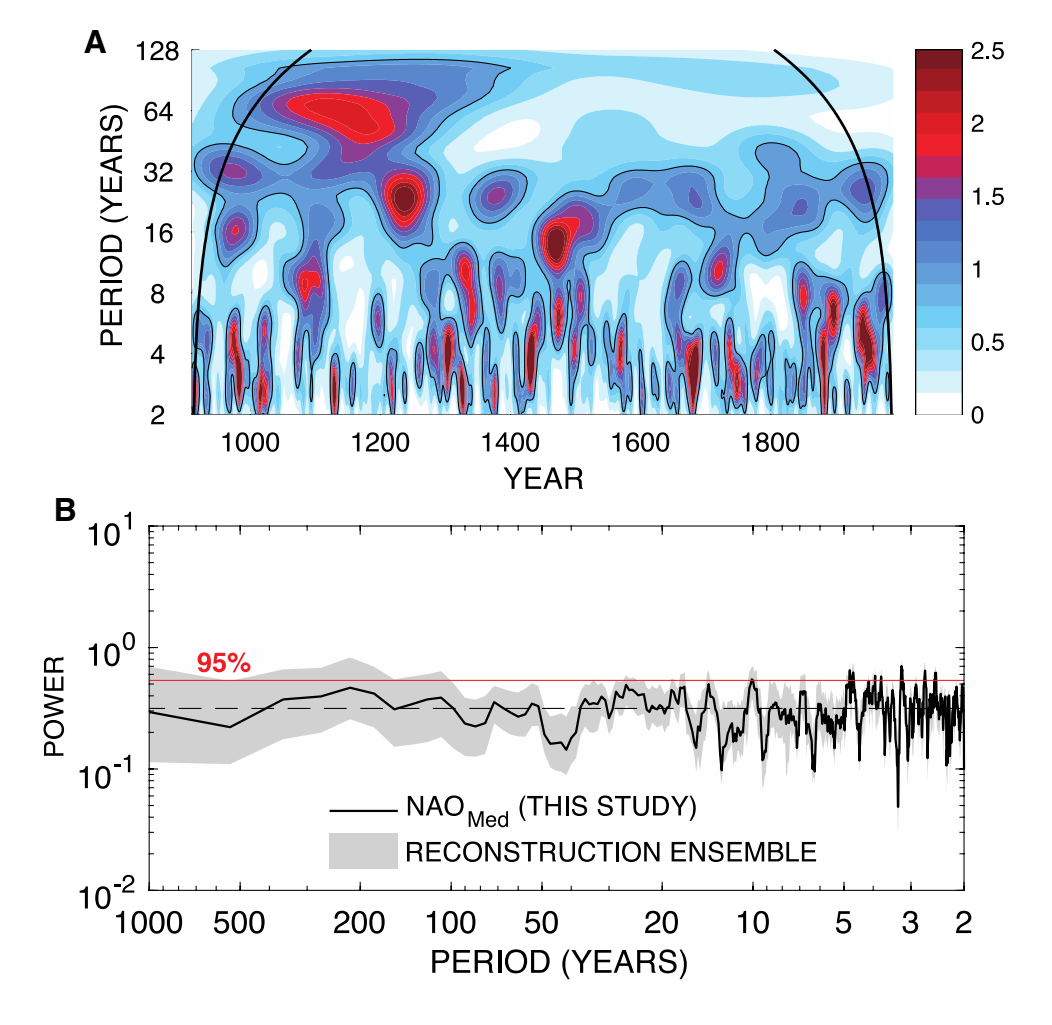
1990 to 2018 with rescaled instrumental NAO indices to match the mean and standard deviation of $\rm NAO_{Med}$ over the 1824–1989 period of overlap. The number of tree-ring chronologies available for each nested reconstruction model is shown in $\bf c$. The minimum number of chronologies used is 25 out of 97 in 910 C.E. Back to 1160 C.E. more than half the total number of chronologies were still available for use



and provide CRSQ and VRSQ statistics for comparison to NAO_{Set} (Table 1). The NAO_{Med} and NAO_{Jones} series covary significantly and have virtually identical CRSQ and VRSQ statistics to those of NAO_{Set} (see the bottom entries in Table 1). We plot the full reconstruction in Fig. 2b, beginning in 910 C.E. with 20-year low-pass spline smoothing applied, along with their smoothed 90% MEB quantile uncertainties. We have also extended NAO_{Med} from 1990 to 2018 with appropriately rescaled instrumental NAO indices based on the early instrumental pressure observations from Gibraltar and Southwest Iceland (Jones et al. 1997). This allows the most recent few decades of winter NAO variability to be compared to estimates over the previous 1000 years. With this in mind, the strongly positive NAO phase between the mid-1960s and mid-1990s (Hurrell and van Loon 1997; Kelley et al. 2012) is highly unusual, but not unprecedented given the reconstructed positive NAO phase found in the 1300s. The number of chronologies used each year in this nested reconstruction is also plotted back to 910 C.E. (Fig. 2c). Because of reduced availability of chronologies back in time, there are a total of 43 nests and the number of chronologies available for each nest ranges from 97 to 25, with more than half available for reconstruction as far back as 1160. Thus, even in the early period of reconstruction the number of available OWDA network chronologies is substantial.

Figure 3 shows the wavelet spectrum (A) (Torrence and Compo 1998) and multi-taper method (MTM) spectrum (B) (Thomson 1982) of the updated NAO_{Med} reconstruction. Examined this way, NAO_{Med} has a broad range of statistically significant (p < 0.1) wavelet power that spans most of the time period since 910 C.E. This includes the expected power in the 2.5 to 10-year band (e.g., Hurrell and van Loon 1997; Gamiz-Fortis et al. 2002). There is also evidence for significant multidecadal to centennial power during the Medieval Climate Anomaly (MCA) period, but the wavelet spectrum shows that it diminishes after entry into the Little Ice Age (LIA) around 1300 C.E. The MTM spectrum shows that overall the NAO_{Med} behaves as and is indistinguishable from a 'white noise' process that contains significant bandlimited variability consistent with the wavelet spectrum. This result differs from that of Wunch (1999) who found the winter NAO spectrum to be slightly red. That analysis was based on a much shorter time period that included persistent

Fig. 3 The wavelet spectrum (a) of the NAO_{Med} reconstruction from 910 to 2018 C.E. based on the Morlet wavelet. Regions in the spectrum bounded by the black contours are statistically significant (p < 0.10), and black curves near the beginning and end of the series indicate the region where padding of the series may influence the spectrum. The 3 to 10-year band has significant, if intermittent, power throughout the past 1109 years. The multidecadal to centennial band of variability is less commonly expressed and mostly restricted to MCA and early LIA periods. The multi-taper method (MTM; 7 4π tapers) spectrum (**b**) reveals that the NAO_{Med} reconstruction effectively behaves as a white noise process (dashed line) with significant (p < 0.1) bandlimited variability similarly represented in the wavelet spectrum. The median reconstruction (black line) does not have any significant power (p > 0.05based on n = 1000 red noise simulations) at multicentennial time scales, while some of the noise-added reconstruction ensemble members do exceed this level





winter NAO variability in the late twentieth century (Hurrell and van Loon 1997), which could reflect anthropogenic forcing by elevated CO_2 and aerosols (Osborn et al. 1999). The much longer perspective provided by the NAO_{Med} reconstruction provides a better estimate of natural NAO variability prior to strong anthropogenic forcing.

Interestingly, the NAO_{Med} wavelet spectrum is qualitatively similar to the wavelet spectrum of a 2000-year stochastic NAO index averaged over the winter (JFM) months (Mecking et al. 2014; their Fig. 3a) and used in model forcing experiments, i.e. their wavelet spectrum has intermittent band-limited behavior like that seen in Fig. 3a. Gómez-Navarro and Zorita (2013) also showed in modeling experiments that internal variability cannot be rejected as the primary source for driving three atmospheric annular modes, including the NAO. The power spectra of 13 model simulations of the NAO driven primarily by solar and volcanic forcing over the past 1000 years were found to be effectively 'white noise' even though the spectrum of the forcing was not, and the smoothed ensemble average of the 13 model simulations evolved through time in a way similar to the 20-year low-pass NAO_{Med} reconstruction in Fig. 2. This indicates no need for external forcing to explain the variability seen in the NAO_{Med} reconstruction.

The MTM spectrum in Fig. 3b does not allow us to reject the hypothesis that the NAO is an internally-forced stochastic process (cf. Gómez-Navarro and Zorita 2013). That said, there are arguments for the NAO being influenced by ocean-atmosphere interactions (e.g., Rodwell et al. 1999; Wang et al. 2006) and even by solar forcing at the 11-year time scale (Thiéblemont et al. 2015; Gray et al. 2016). Regarding the latter, Gray et al. (2016) report that there is a "tendency for positive NAO anomalies to follow solar maxima and negative NAO anomalies to follow solar minima", with the peak response lagged by about 4 years. The MTM spectrum (Fig. 3b) of NAO_{Med} does have a small, but significant (p < 0.10), spectral peak at the ~ 11 period that is consistent with solar forcing, but cross-wavelet analysis (not shown) does not reveal consistent temporal phase coherence between the NAO_{Med} and solar forcing. A more recent evaluation of the link between the 11-year solar cycle and the winter NAO also failed to find a meaningful link between them (Chiodo et al. 2019). Such inconsistency between solar forcing and the reconstructed NAO is likewise apparent for grand solar minima as well: our reconstruction is consistently low during the Dalton minimum near 1800, but there is no evident response during the Maunder Minimum, ca. 1645 to 1715.

3.2 NAO reconstruction comparisons

NAO_{Med} extends back to 910 C.E. and covers most of the MCA, making it the longest annually resolved reconstruction

of the NAO known to the authors. At this point it is worth comparing NAO $_{\rm Med}$, NAO $_{\rm Ortega}$, and NAO $_{\rm Cook}$ more closely. NAO $_{\rm Trouet}$ has not been evaluated up to this point because it is highly smoothed due to its use of the speleothem record from Scotland and, therefore, could not be used in comparative calibration/validation testing as done with NAO $_{\rm Med}$, NAO $_{\rm Ortega}$, and NAO $_{\rm Cook}$ (Table 2).

Figure 4 shows the NAO_{Med}, NAO_{Ortega}, NAO_{Cook}, and NAO_{Trougt} series plotted over their full lengths. They have been normalized by their respective means and standard deviations over the common 1400–1969 period to facilitate visual comparisons. Additionally, each normalized series has had a 50-year low-pass filter applied to highlight multidecadal variability, with NAO_{Trougt} being only slightly more smoothed than its original 30-year low-pass filtered version. Visually, there are notable differences between the annuallyresolved reconstructions. NAO_{Med} and NAO_{Cook} are dominated by high-frequency variability. They are also significantly correlated (r = 0.50) at 50-year high-pass time scales over the common period, likely due in part to some shared tree-ring data in Europe. In contrast, NAO_{Ortega} has more low-frequency variability that is highly correlated (r=0.84)with NAO_{Troug} at periods > 50 years. This high correlation likely partially reflects the use of similarly sourced speleothem data from Scotland.

Before 1400, interesting differences between NAO_{Med}, NAO_{Ortega}, and NAO_{Trouet} are evident. Both NAO_{Ortega} and NAO_{Trouet} are positive during the MCA, but the amplitude of the NAO_{Ortega} positive anomaly is far smaller than that of NAO_{Trouet} and falls within its reconstruction uncertainties (see Fig. 2b in Ortega et al. 2015). NAO_{Med} differs even more from the others with its weakly negative pattern of NAO variability during the MCA, especially from 1090 to 1300, but this difference likewise falls within its reconstruction uncertainties (Fig. 2a). Thus, neither NAO_{Med} nor NAO_{Ortega} support the persistent positive NAO mode during the MCA reported by Trouet et al. (2009), a conclusion similar to that of Ortega et al. (2015). In contrast, the speleothem evidence presented by Wassenburg et al. (2013), Baker et al. (2015), and Deininger et al. (2017) continues to support the finding of Trouet et al. (2009). This difference between NAO reconstructions suggests that the speleothem records are recording a different expression of North Atlantic climate variability and/or are affected by proxy-specific processes that result in a redder climate signal (Jones et al. 2003; Evans et al. 2013).

The visible difference in time series persistence between NAO_{Med} and NAO_{Ortega} (Fig. 4) is expressed clearly in their power spectra (Fig. 5a). With its lower relative variance at higher frequencies and resulting inflation of variance at lower frequencies, the NAO_{Ortega} power spectrum behaves more like a 'red noise' process than a 'white noise' process (sensu Gilman et al. 1963). In comparison, the relatively



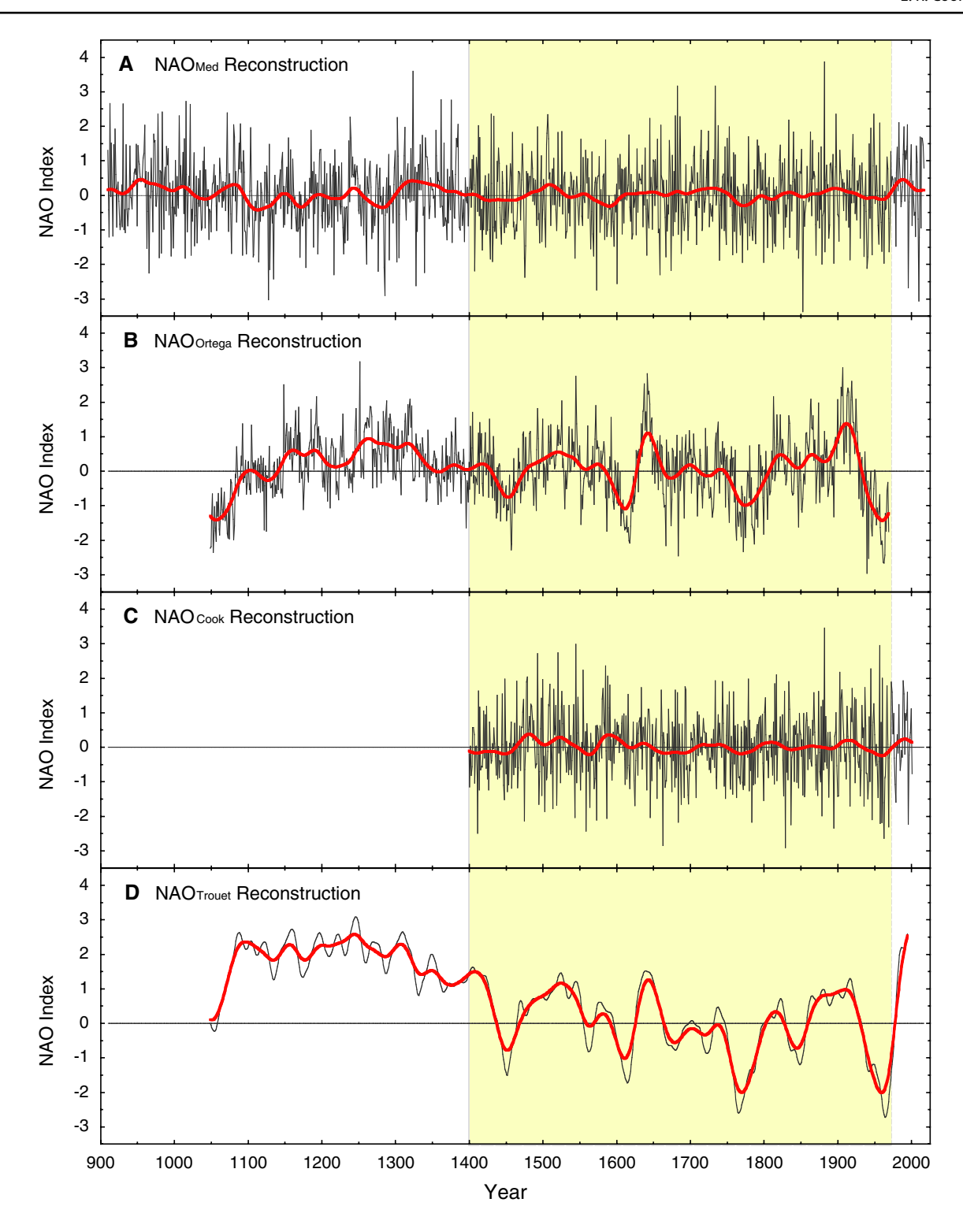


Fig. 4 Four winter NAO reconstructions compared in this study: **a** NAO $_{Med}$, **b** NAO $_{Ortega}$, **c** NAO $_{Cook}$, **d** NAO $_{Trouel}$; as defined in text. The series have been normalized using their respective means and standard deviations estimated over the common periods from 1400

to 1969 (highlighted in yellow) to facilitate visual comparisons. Each reconstruction (black) also has been smoothed with a 50-year low-pass smoothing spline (red) to highlight multidecadal variability



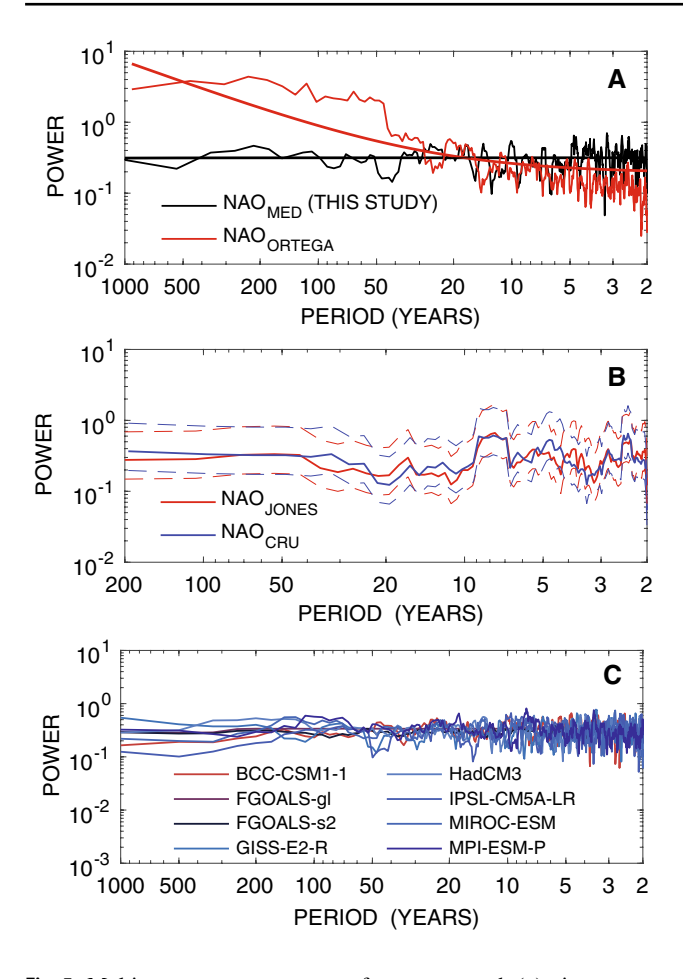


Fig. 5 Multi-taper power spectra of reconstructed (a), instrumental (b), and (c) Last Millennium+historical PMIP3/CMIP5 model simulated winter NAO indices. Seven 4π tapers were applied in estimating all power spectra. The MTM power spectra of NAO_{Med} and NAO_{Ortega} were based on the 1049 to 1969 time period in common. The MTM power spectra of NAO_{Jones} and NAO_{CRU} are based on their 1781-1995 and 1824-2018 time periods, respectively, to enable the longest overall time span of instrumental data to be evaluated. Model simulations are over their full length (typically 850 to 2005) and models with multiple ensemble members were averaged. In a the red and black slopes of the spectra were estimated by least squares. In b dashed lines show the 95% confidence interval for the spectral estimate. Comparison of the spectral slopes reveals that only NAO_{Ortega} differs from that expected for a 'white noise' process, i.e., the power spectra of $\rm NAO_{Med},\, NAO_{Jones},$ and $\rm NAO_{CRU}$ are 'flat'. In contrast, the strongly negative slope of the NAO_{Ortega} spectrum is characteristic of a 'red noise' process

even distribution of variance as a function of frequency in the NAO_{Med} spectrum is similar to that expected from a stochastically forced 'white noise' process (Mecking et al. 2014).

Given these differences in overall spectral shape, which 'noise model' is more likely to be correct for the winter NAO? One way to investigate this is to compare the power spectra of the reconstructions to those of the long instrumental NAO $_{\rm Jones}$ and NAO $_{\rm CRU}$ indices shown in Fig. 1. NAO $_{\rm Jones}$

and NAO_{CRU} are direct estimates of winter NAO variability based on the SLP difference between Gibraltar and Southwest Iceland. Thus, their spectra should be representative of the 'true' spectral shape of this atmospheric pressure index back to at least 1781. Other estimates of winter NAO variability based on a mixture of climate data types (e.g., the temperature and precipitation data used in NAO_{Lut1}; Luterbacher et al. 2002a) are likely to introduce other sources of variability into the power spectrum due to surface climate effects (Jones et al. 2003). In fact, the spectrum of NAO_{Lut1} (not shown) has significantly more redness in its power spectrum compared to NAO_{Iones}, which is arguably a direct consequence of surface climate effects in the NAO_{Lut1} that are less strongly related to direct NAO forcing. For this reason, only NAO_{Iones} and NAO_{CRII} are used for comparison herein because they are based strictly on SLP data.

The NAO_{Jones} and NAO_{CRU} power spectra are shown in Fig. 5b. They are extremely similar to each other given how highly correlated these series are (Fig. 1), and they behave overall as 'white noise' processes. Additionally, the spectra of NAO_{Jones} and NAO_{CRU} compare far better to the spectrum of NAO_{Med} than to that of NAO_{Ortega}. This indicates that NAO_{Med} is likely to be the more appropriate expression of winter NAO variability than NAO_{Ortega} over time. This determination is further supported by the power spectra of winter NAO variability estimated from the Last Millennium+Historical PMIP3/CMIP5 model simulations (Taylor et al. 2012). These spectra are again consistent with the NAO being a stochastically forced process, a result that agrees with the findings of Gómez-Navarro and Zorita (2013) as well.

Finally, four statistical methods of climate mode reconstruction from proxies were recently investigated by Michel et al. (2018), with the winter NAO index serving as the experimental target variable. These experiments were based on quite different suites of proxy data than used here. Among the methods tested was the PCR method applied herein. Across the four tested methods, Michel et al. (2018) did not find any one to be superior, but the reconstructions produced by their four methods resulted in outcomes that were visually more similar to the NAO reconstruction developed herein than to the Ortega et al. (2015) reconstruction.

4 Conclusions

The extended winter NAO_{Med} reconstruction produced herein is a new and well-validated estimate of long-term atmospheric variability and forcing over the North Atlantic. It is based on the same tree-ring chronology network used to reconstruct the Old World Drought Atlas (Cook et al. 2015), which is strongly associated with winter NAO impacts on hydroclimate over Europe and the Mediterranean region



that extend into the summer months. Nested correlation-weighted PCR is the employed method of reconstruction, while the MEB was used to generate a 2400-member ensemble of reconstructions for estimating the final reconstruction and its quantile uncertainties. The NAO_{Med} reconstruction has also been updated with appropriately rescaled CRU instrumental DJFM NAO indices and covers the period 910–2018 C.E.

The usefulness of NAO_{Med} for analysis and modeling is indicated by its documented skill and its ability to reproduce the basic 'white noise' spectral properties of the instrumental winter NAO index since 1781. This property differentiates it from the more 'red noise' character of the NAO_{Ortega} reconstruction. The added persistence in NAO Ortega may originate from the inclusion of speleothem data that integrate and redden surface climate effects in complex ways due to the heterogeneity of groundwater flow in the aquifer above the cave where the speleothem is growing (Fairchild et al. 2006; Truebe et al. 2010; Evans et al. 2013; Dee et al. 2015). The concerns of Jones et al. (2003) about surface climate effects modifying the expression of NAO variability in non-SLP data are therefore relevant. It is also possible that the speleothems are recording a somewhat different expression or time scale of North Atlantic climate variability than that captured in the tree rings.

The overall 'white noise' property of NAO_{Med} suggests that there is no need for external forcing to generate the intermittent band-limited patterns of variability found within it, as indicated by the wavelet and MTM spectra. Such variability could arise from stochastic forcing alone (Mecking et al. 2014). However, it is still possible that some level of oceanic (or even solar) forcing could yet be a contributor to the variability found in the NAO_{Med} reconstruction and this requires further exploration. The wavelet spectrum indicates that reconstructed winter NAO variability has consistent, if somewhat intermittent, band-limited power at periods of 3–11 years over the entire 1109 years of reconstruction. There is also some evidence of multidecadal to centennial power in the reconstruction, but it is mostly limited to the MCA and early LIA.

Regarding the behavior of the winter NAO during the MCA, little can be definitively said from the results presented herein, with the exception that our results clearly differ from the persistently positive NAO_{Trouet} result during this period. NAO_{Med} is weakly negative during the MCA, especially from 1090 to 1300, and NAO_{Ortega} is weakly positive around the same time. Unfortunately, the uncertainties of both NAO_{Med} and NAO_{Ortega} are too large to confidently determine if either is more correct than the other during the MCA. Thus, efforts to more precisely reconstruct and characterize the behavior of the winter NAO on an interannual basis during the MCA must continue before any firm conclusions can be made.

Acknowledgements This research is supported by National Science Foundation Grant nos AGS-1501856, AGS-1734760, and AGS-1703029. We also acknowledge the World Climate Research Programme's Working Group on Coupled Modelling, which is responsible for CMIP, and we thank the climate modeling groups for producing and making available their model output. The CMIP5 data used here was archived and served from the IRI/LDEO Climate Data Library. Lamont-Doherty Earth Observatory Contribution No. 8295.

References

- Appenzeller C, Stocker TF, Anklin M (1998) North Atlantic Oscillation dynamics recorded in Greenland ice cores. Science 282:446–449
- Baek SH, Smerdon JE, Coats S, Williams AP, Cook BI, Cook ER, Seager R (2017) Precipitation, temperature, and teleconnection signals across the combined North American, Monsoon Asia, and Old World Drought Atlases. J Clim 30:7141–7155
- Baker A, Hellstrom C, Kelly BF, Mariethoz G, Trouet V (2015) A composite annual-resolution stalagmite record of North Atlantic climate over the last three millennia. Sci Rep 5:10307. https://doi. org/10.1038/srep10307
- Barnston AG, Livezey RE (1987) Classification, seasonality and persistence of low-frequency atmospheric circulation patterns. Mon Wea Rev 115:1083–1126
- Berk KN (1984) Validating regression procedures with new data. Technometrics 26(4):331–338
- Chiodo G, Oehrlein J, Polvani LM (2019) Insignificant influence of the 11-year solar cycle on the North Atlantic Oscillation. Nat Geo. https://doi.org/10.1038/s41561-018-0293-3
- Cook BI, Buckley BM (2009) Objective determination of monsoon season onset, withdrawal, and length. J Geophys Res 114(D23):D23109. https://doi.org/10.1029/2009JD012795
- Cook ER, Meko DM, Stahle DW, Cleaveland MK (1999) Drought reconstructions for the continental United States. J Clim 12:1145–1162
- Cook ER, D'Arrigo RD, Briffa KR (1998) A reconstruction of the North Atlantic Oscillation using tree-ring chronologies from North America and Europe. Holocene 8(1):9–17
- Cook ER, Anchukaitis KJ, Buckley BM, D'Arrigo RD, Jacoby GC, Wright WE (2010) Asian monsoon failure and megadrought during the last millennium. Science 328(5977):486–489
- Cook ER, D'Arrigo RD, Mann ME (2002) A well-verified, multi-proxy reconstruction of the winter North Atlantic oscillation index since AD 1400. J Clim 15(13):1754–1764
- Cook ER, Palmer JG, Ahmed M, Woodhouse CA, Fenwick P, Zafar MU, Wahab M, Khan N (2013a) Five centuries of upper Indus River flow from tree rings. J Hydrol 486:365–375
- Cook ER, Krusic PJ, Anchukaitis KJ, Buckley BM, Nakatsuka T, Sano M, Asia2k members (2013b) Tree-ring reconstructed summer temperature anomalies for temperate East Asia since 800 C.E. Clim Dyn 41:2957–2972. https://doi.org/10.1007/s00382-012-1611-x
- Cook ER, Seager R, Kushnir J, Briffa KR, Buentgen U, Frank D, Krusic PJ, Tegel W, van der Schrier G, Andreu-Hayles L, Baillie M, Baitttinger C, Bleicher N, Bonde N, Brown D, Carrer M, Cooper R, Cufar K, Dittmar C, Esper J, Griggs C, Gunnarson B, Gunther B, Gutierrez E, Haneca K, Helema S, Herzig F, Heussner K-U, Hofmann J, Janda J, Kontic R, Kose N, Kyncl T, Levanic T, Linderholm H, Manning S, Melvin T, Miles D, Neuwirth B, Nicolussi K, Nola P, Panayotov M, Popa I, Rothe A, Seftigen K, Seim A, Svarva H, Svoboda M, Thun T, Timonen M, Touchan R, Trotsiuk V, Trouet V, Walder F, Wazny T, Wilson R, Zang C (2015) Old world megadroughts and pluvials during the Common Era. Sci Adv 1(10):e1500561. https://doi.org/10.1126/sciadv.1500561



- Cornes RC, Jones PD, Briffa KR, Osborn TJ (2013) Estimates of the North Atlantic Oscillation back to 1692 using a Paris-London westerly index. Int J Clim 33:228-248
- Cullen H, D'Arrigo R, Cook E, Mann ME (2001) Multiproxy-based reconstructions of the North Atlantic Oscillation over the past three centuries. Paleoceanography 15:27–39
- Dee S, Emile-Geay J, Evans MN, Allam A, Steig EJ, Thompson DM (2015) PRYSM: an open-source framework for PRoxY system modeling, with applications to oxygen-isotope systems. J Adv Mod Earth Sys 7:1220–1247. https://doi.org/10.1002/2015M S000447
- Deininger M, McDermott F, Mudelsee M, Werner M, Frank N, Mangini A (2017) Coherency of late holocene European speleothem δ¹⁸O records linked to North Atlantic Ocean circulation. Clim Dyn 49:595–618
- Dong B, Sutton RT, Woollings T (2011) Changes of interannual NAO variability in response to greenhouse gases forcing. Clim Dyn 37:1621–1641
- Efroymson MA (1960) Multiple regression analysis. In: Ralston A, Wilf HS (eds) Mathematical methods for digital computers. Wiley, New York
- Esper J, Frank D, Buentgen U, Verstege A, Luterbacher J, Xoplaki E (2007) Long-term drought severity variations in Morocco. Geophys Res Lett 34:L17702. https://doi.org/10.1029/2007GL030844
- Evans MN, Tolwinski-Ward SE, Thompson DM, Anchukaitis KJ (2013) Applications of proxy system modeling in high resolution paleoclimatology. Quat Sci Rev 76:16–28. https://doi.org/10.1016/j.quascirev.2013.05.024
- Fairchild IJ, Smith CL, Baker A, Fuller L, Spötl C, Mattey D, McDermott F (2006) Modification and preservation of environmental signals in speleothems. Earth-Sci Rev 75(1-4):105-153
- Gamiz-Fortis SR, Pozo-Vazquez D, Esteban-Parra MJ, Castro-Diez Y (2002) Spectral characteristics and predictability of the NAO assessed through singular spectral analysis. J Geophys Res 107(D23):4685. https://doi.org/10.1029/2001JD001436
- García-Suáreza AM, Butler CJ, Baillie MGL (2009) Climate signal in tree-ring chronologies in a temperate climate: a multi-species approach. Dendrochronologia 27:183–198
- Gilman DL, Fuglister FJ, Mitchell JM Jr (1963) On the power spectrum of 'red noise'. J Atmos Sci 20(2):182–184
- Gómez-Navarro JJ, Zorita E (2013) Atmospheric annular modes in simulations over the past millennium: no long-term response to external forcing. Geophys Res Lett 40:3232–3236. https://doi.org/10.1002/grl.50628
- Gray LJ, Woollings TJ, Andrews M, Knight J (2016) Eleven-year solar cycle signal in the NAO and Atlantic/European blocking. Quart J Royal Meterol Soc 142:1890–1903
- Hurrell JW (1995) Decadal trends in the North Atlantic Oscillation: regional temperatures and precipitation. Science 269:676–679
- Hurrell JW, Deser C (2009) North Atlantic climate variability: The role of the North Atlantic Oscillation. J Marine Sys 78:28–41
- Hurrell JW, van Loon H (1997) Decadal variations in climate associated with the North Atlantic Oscillation. Clim Change 36:301–326
- Hurrell JW, Kushnir Y, Visbeck M, Ottersen G (2003) An overview of the North Atlantic Oscillation. In Hurrell JW, Kushnir Y, Otterson G, Visbeck MH (eds) The North Atlantic Oscillation. AGU Geophysical Monograph, New York, vol 134, pp1–35
- Jones PD, Jónsson T, Wheeler D (1997) Extension to the North Atlantic Oscillation using early instrumental pressure observations from Gibraltar and South-West Iceland. Int J Clim 17:1433–1450
- Jones PD, Davies TD, Lister DH, Slonosky V, Jonsson T, Barring L, Jonsson P, Maheras P, Kolyva-Machera F, Barriendos M, Martin-Vide J, Rodrigue R, Alcoforado MJ, Wanner H, Pfister C, Luterbacher J, Rickli R, Schuepbach E, Kaas E, Schmith T, Jacobeit J, Beck C (1999) Monthly mean pressure reconstructions for Europe for the 1780–1995 period. Int J Clim 19:347–364

- Jones PD, Osborn TJ, Briffa KR (2003) Pressure-based measures of the North Atlantic Oscillation (NAO): a comparison and an assessment of changes in the strength of the NAO and in its influence on surface climate parameters. In Hurrell JW, Kushnir Y, Otterson G, Visbeck MH (eds) The North Atlantic Oscillation. AGU Geophysical Monograph, New York, vol 134, pp 51-62
- Kelley C, Ting MF, Seager R, Kushnir Y (2012) The relative contributions of radiative forcing and internal climate variability to the late 20th Century winter drying of the Mediterranean region. Clim Dyn 38(9–10):2001–2015
- Lopez-Moreno JI, Vicente-Serrano SM (2008) Positive and negative phases of the wintertime North Atlantic Oscillation and drought occurrence over Europe: a multitemporal-scale approach. J Clim 21:1220–1243
- Luterbacher J, Schmutz C, Gyalistras D, Xoplaki E, Wanner H (1999) Reconstruction of monthly NAO and EU indices back to AD 1675. Geophys Res Lett 26:2745–2748
- Luterbacher J, Xoplaki E, Dietrich D, Jones PD, Davies TD, Portis D, Gonzalez-Rouco JF, von Storch H, Gyalistris D, Casty C, Wanner H (2002a) Extending North Atlantic Oscillation reconstructions back to 1500. Atmos Sci Lett 2:114–124. https://doi.org/10.1006/ asle.2001.0044
- Luterbacher J, Xoplaki E, Dietrich D, Rickli R, Jacobeit J, Beck C, Gyalistras D, Schmutz C, Wanner H (2002b) Reconstruction of sea level pressure fields over the Eastern North Atlantic and Europe back to 1500. Clim Dyn 18:545–561
- Mecking JV, Keenlyside NS, Greatbatch RJ (2014) Stochasticallyforced multidecadal variability in the North Atlantic: a model study. Clim Dyn 43:271–288
- Meko DM (1981) Applications of Box-Jenkins methods of time series analysis to the reconstruction of drought from tree rings. Dissertation, University of Arizona
- Michel S, Swingedouw D, Chavent M, Ortega P, Mignot J, Khodri M (2018) Reconstructing climatic modes of variability from proxy records: sensitivity to the methodological approach. Geosci Model Dev Discuss. https://doi.org/10.5194/gmd-2018-211
- Olive DJ (2007) Prediction intervals for regression models. Comp Stat Data Anal 51:3115–3122
- Ortega P, Lehner F, Swingedouw D, Masson-Delmotte V, Raible CC, Casado M, Yiou P (2015) A model-tested North Atlantic Oscillation reconstruction for the past millennium. Nature 523:71–74. https://doi.org/10.1038/nature14518
- Osborn TJ (2004) Simulating the winter North Atlantic Oscillation: the roles of internal variability and greenhouse gas forcing. Clim Dyn 22:605–623
- Osborn TJ, Briffa KR, Tett SFB, Jones PD, Trigo RM (1999) Evaluation of the North Atlantic Oscillation as simulated by a coupled climate model. Clim Dyn 15:685–702
- Palmer JG, Cook E, Turney C, Allen K, Fenwick P, Cook B, O'Donnell A, Lough J, Grierson P, Baker P (2015) Drought variability in the eastern Australia and New Zealand summer drought atlas (ANZDA, CE 1500–2012) modulated by the Interdecadal Pacific Oscillation. Env Res Lett. https://doi.org/10.1088/1748-9326/10/12/124002
- Pederson N, Bell AR, Cook ER, Lall U, Devineni N, Seager R, Eggelston K, Vranes KJ (2013) Is an epic pluvial masking the water security of the greater New York City region? J Clim 26:1339–1354. https://doi.org/10.1175/JCLI-D-11-00723.1
- Proctor CJ, Baker A, Barnes WL, Gilmour MA (2000) A thousand year speleothem proxy record of North Atlantic climate from Scotland. Clim Dyn 16(10–11):815–820
- Rao MP, Cook ER, Cook BI, Palmer J, Uriarte M, Devineni N, Lall U, D'Arrigo RD, Woodhouse CA, Ahmed M (2018) Six centuries of Upper Indus Basin streamflow variability and its climatic drivers. Water Resourc Res. https://doi.org/10.1029/2018WR023080



- Rind D, Perlwitz J, Lonergan P, Lerner J (2005) AO/NAO response to climate change: 2. Relative importance of low and high latitude temperature changes. J Geophys Res 110:D12108. https://doi. org/10.1029/2004JD005686
- Rodwell MJ, Rowell DP, Folland CK (1999) Oceanic forcing of the wintertime North Atlantic Oscillation and European climate. Nature 398:320–323
- Rogers JC, van Loon H (1979) The seesaw in winter temperatures between Greenland and northern Europe. Part II: some oceanic and atmospheric effects in middle and high latitudes. Mon Wea Rev 107:509–519
- Schmidt GA, Jungclaus JH, Ammann CM, Bard E, Braconnot P, Crowley TJ, Delaygue G, Joos F, Krivova NA, Muscheler R, Otto-Bliesner BL, Pongratz J, Shindell DT, Solanki SK, Steinhilber F, Vieira LEA (2012) Climate forcing reconstructions for use in PMIP simulations of the Last Millennium (v1.1). Geosci Mod Dev 5:185–191. https://doi.org/10.5194/gmd-5-185-2012
- Schmutz C, Luterbacher J, Gyalistras D, Xoplaki E, Wanner H (2000) Can we trust proxy-based NAO index reconstructions? Geophys Res Lett 27:1135–1138
- Smerdon JE, Cook BI, Cook ER, Seager R (2015) Bridging past and future climate across paleoclimatic reconstructions, observations, and models: A hydroclimate case study. J Clim 28(8):3212–3231
- Srivastav RK, Simonovic SP (2015) Multi-site, multivariate weather generator using maximum entropy bootstrap. Clim Dyn 44:3431–3448
- Stahle DW, Cook ER, Burnette DJ, Villanueva J, Cerano J, Burns JN, Griffin RD, Cook BI, Acuna R, Torbenson MCA, Sjezner P (2016) The Mexican drought atlas: tree-ring reconstructions of the soil moisture balance during the last pre-Hispanic, colonial, and modern eras. Quat Sci Rev 149:34–60
- Stephenson DB, Wanner H, Bronnimann S, Luterbacheer J (2003) The history of scientific research on the North Atlantic Oscillation. In Hurrell JW, Kushnir Y, Otterson G, Visbeck MH (eds) The North Atlantic Oscillation. AGU Geophysical Monograph, New York, vol 134, pp 37–50
- Stockton CW, Glueck MF (1999) Long-term variability of the North Atlantic Oscillation (NAO). In: American Meteorological Society I0th Symposium on Global Change Studies, Dallas, Texas, pp 290–293
- Taylor KE. Stouffer RJ. Meehl GA (2012) An overview of CMIP5 and the experiment design. Bull Am Meterol Soc 93:485–498. https://doi.org/10.1175/BAMS-D-11-00094.1
- Thiéblemont R, Matthes K, Omrani N-E, Kodera K, Hansen F (2015) Solar forcing synchronizes decadal North Atlantic climate variability. Nature Comm 6:8268. https://doi.org/10.1038/ncomms9268
- Thomson DJ (1982) Spectrum estimation and harmonic analysis. Proc IEEE 70:1055–1096
- Tierney JE, Abram NJ, Anchukaitis KJ, Evans MN, Giry C, Kilbourne KH, Saenger CP, Wu HC, Zinke J (2015) Tropical sea surface temperatures for the past four centuries reconstructed

- from coral archives. Paleoceanography 30:226–252. https://doi.org/10.1002/2014PA002717
- Torrence C, Compo GP (1998) A practical guide to wavelet analysis. Bull Am Meterol Soc 79(1):61–78
- Trigo RM, Osborn TJ, Corte-Real JM (2002) The North Atlantic Oscillation influence on Europe: climate impacts and associated physical mechanisms. Clim Res 20:9–17
- Trouet V, Esper J, Graham NE, Baker A, Scourse JD, Frank DC (2009) Persistent positive North Atlantic oscillation mode dominated the Medieval Climate Anomaly. Science 324:78–80. https://doi. org/10.1126/science.1166349
- Truebe S, Ault TR, Cole JE (2010) A forward model of cave dripwater δ¹⁸O and application to speleothem records. IOP Conf Ser Earth Environ Sci. https://doi.org/10.1088/1755-1315/9/1/012022
- van Loon H, Rogers JC (1978) The seesaw in winter temperatures between Greenland and northern Europe. Part I: general description. Mon Wea Rev 106:296–310
- Vinod HD (2006) Maximum entropy ensembles for time series inference in economics. J Asian Econ 17:955–978
- Wahl E, Ammann C (2007) Robustness of the Mann, Bradley, Hughes reconstruction of Northern Hemisphere surface temperatures: examination of criticisms based on the nature and processing of proxy climate evidence. Clim Change 85:33–69. https://doi. org/10.1007/s10584-006-9105-7
- Wallace J, Gutzler D (1981) Teleconnections in the geopotential height field during the Northern Hemisphere winter. Mon Wea Rev 109:784–812
- Wang W, Anderson BT, Kaufmann RK, Myneni RB (2006) The relation between the North Atlantic Oscillation and SSTs in the North Atlantic basin. J Clim 17:4752–4759
- Wassenburg JA, Immenhauser A, Richter DK, Niedermayr A, Riechelmann S, Fietzke J, Scholz D, Jochum KP, Fohlmeister J, Schroder-Ritzrau A, Sabaoui A, Riechelmann DFC, Schneider L, Esper J (2013) Moroccan speleothem and tree ring records suggest a variable positive state of the North Atlantic Oscillation during the Medieval Warm Period. Earth Planet Sci Lett 375:291–302
- Wonnocott RJ, Wonnocott TH (1979) Econometrics, 2 ed. Wiley, Hoboken
- Woollings T, Franzke C, Hodson DLR, Dong B, Barnes EA, Raible CC, Pinto JG (2015) Contrasting interannual and multidecadal NAO variability. Clim Dyn 45(1):539–556
- Wunch C (1999) The interpretation of short climate records, with comments on the North Atlantic and Southern Oscillations. Bull Am Meteorol Soc 80(2):245–255

Publisher's Note Springer Nature remains neutral with regard to jurisdictional claims in published maps and institutional affiliations.

